

Mantle thermal structure and active upwelling during continental breakup in the North Atlantic

W. Steven Holbrook^{a,*}, H.C. Larsen^b, J. Korenaga^c, T. Dahl-Jensen^b,
I.D. Reid^b, P.B. Kelemen^d, J.R. Hopper^b, G.M. Kent^e, D. Lizarralde^f,
S. Bernstein^b, R.S. Detrick^d

^a Department of Geology and Geophysics, University of Wyoming, Laramie, WY 82071-3006, USA

^b Danish Lithosphere Centre, Øster Voldgade 10, DK1350 Copenhagen, Denmark

^c Department of Earth, Atmospheric and Planetary Sciences, Massachusetts Institute of Technology, Cambridge, MA 02139, USA

^d Department of Geology and Geophysics, Woods Hole Oceanographic Institution, Woods Hole, MA 02543-1542, USA

^e Scripps Institution of Oceanography, University of California, San Diego, La Jolla, CA 92093-0225 USA

^f School of Earth and Atmospheric Sciences, Georgia Institute of Technology, 221 Bobby Dodd Way, Atlanta, GA 30332, USA

Received 11 June 2000; received in revised form 1 June 2001; accepted 2 June 2001

Abstract

Seismic reflection and refraction data acquired on four transects spanning the Southeast Greenland rifted margin and Greenland–Iceland Ridge (GIR) provide new constraints on mantle thermal structure and melting processes during continental breakup in the North Atlantic. Maximum igneous crustal thickness varies along the margin from > 30 km in the near-hotspot zone (< 500 km from the hotspot track) to ~ 18 km in the distal zone (500–1100 km). Magmatic productivity on summed conjugate margins of the North Atlantic decreases through time from 1800 ± 300 to 600 ± 50 km³/km/Ma in the near-hotspot zone and from 700 ± 200 to 300 ± 50 km³/km/Ma in the distal zone. Comparison of our data with the British/Faeroe margins shows that both symmetric and asymmetric conjugate volcanic rifted margins exist. Joint consideration of crustal thickness and mean crustal seismic velocity suggests that along-margin changes in magmatism are principally controlled by variations in active upwelling rather than mantle temperature. The thermal anomaly (ΔT) at breakup was modest (~ 100 – 125°C), varied little along the margin, and transient. Data along the GIR indicate that the potential temperature anomaly ($125 \pm 50^\circ\text{C}$) and upwelling ratio (~ 4 times passive) of the Iceland hotspot have remained roughly constant since 56 Ma. Our results are consistent with a plume–impact model, in which (1) a plume of radius ~ 300 km and ΔT of $\sim 125^\circ\text{C}$ impacted the margin around 61 Ma and delivered warm material to distal portions of the margin; (2) at breakup (56 Ma), the lower half of the plume head continued to feed actively upwelling mantle into the proximal portion of the margin; and (3) by 45 Ma, both the remaining plume head and the distal warm layer were exhausted, with excess magmatism thereafter largely confined to a narrow (< 200 km radius) zone immediately above the Iceland plume stem. Alternatively, the warm upper mantle layer that fed excess magmatism in the distal portion of the margin may have been a pre-existing thermal anomaly unrelated to the plume. © 2001 Elsevier Science B.V. All rights reserved.

Keywords: volcanism; rift zones; refraction methods; large igneous provinces; North Atlantic

* Corresponding author. Tel.: +1-307-766-2427; Fax: +1-307-766-6679. E-mail address: steveh@uwyo.edu (W.S. Holbrook).

1. Introduction

When a continent ruptures, prodigious volcanism can occur, producing enormous volumes of igneous rocks in an elongate magmatic province extending along the entire rifted edge of the continent (e.g., [1–3]). These volcanic rifted margins (VRM) are the dominant type of rifted margin in the Atlantic (e.g., [4–6]), but the cause of the anomalous volcanism is poorly understood. The igneous crust emplaced at VRM has three distinguishing geophysical characteristics. First, its lower crust has high P-wave velocities (> 7.2 km/s), suggesting compositions more mafic than normal oceanic lower crust [3,7]. Second, seismic reflection data over VRM show wedges of seaward-dipping reflection sequences (SDRS, [1,8]) that correspond to subaerially deposited basalt flows [9–11]. Third, VRM crust often exceeds 20 km in thickness – more than three times as thick as normal oceanic crust, which is produced by passively upwelling mantle [12] with a potential temperature of about 1280°C [13,14]. VRM production thus requires mantle that is anomalously warm [3], anomalously fertile, actively upwelling [15,16], or some combination thereof [7].

The margins of the North Atlantic have played a key role in the development of ideas regarding VRM genesis. Breakup of Greenland from northern Europe about 56 Ma left behind massive sequences of igneous rocks, including flood basalts on Greenland, the Faeroe Islands, and Great Britain (e.g., [17,18]) and SDRS that extend at least 2600 km along strike (e.g., [2,4,8,19–21]). The apparent association of North Atlantic VRM and the Iceland hotspot led to the hypothesis that VRM are the expression of hot mantle temperatures resulting from a mantle plume. Various plume structures at VRM have been proposed, including steady-state incubating plume heads [22], large mushroom heads of impacting plumes [23,24], and rising, vertical sheets [25,26]. Alternatively, it has been proposed that (1) hot material derived from plumes ponds beneath thick continental lithosphere over a wide region prior to rifting [27], (2) a hot mantle reservoir develops below continental lithosphere independently of plumes [28,29], or (3) rifting itself instigates active mantle

upwelling and a melting anomaly without a significant temperature anomaly (e.g., [15,16]).

Three questions crucial to examining any of the above hypotheses are: (1) What was the magnitude of the mantle temperature anomaly, if any, during breakup? (2) Did active upwelling of the mantle take place? And (3) how did the thermal anomaly and active upwelling vary in time and space? (We define active upwelling in a purely kinematic sense, where the upwelling rate of mantle through the melting zone exceeds the half-spreading rate of the rift. Passive upwelling, in contrast, is considered as simple corner flow in which the upwelling rate equals the half-spreading rate. This definition of active upwelling differs from the common usage in the mid-ocean ridge literature, in which retained melt is invoked to enhance buoyancy [30,31]. Because continental rifting is a transient process, decoupling of mantle flow from surface motion is viable; our active upwelling ratio is designed to quantify that decoupling.) Understanding the spatial and temporal variation of mantle temperature and active upwelling along the evolving margin would place strong constraints on models of rift dynamics, plume–rift interaction, and rift-related convection. In particular, we need tests that might distinguish between models that invoke high mantle temperatures with passive upwelling (e.g., 1550°C; [26]), no thermal anomalies but strongly active upwelling (e.g., [16]), and more recent models that combine modest mantle temperatures and active upwelling (e.g., [32,33]).

Data from the SIGMA study (SIGMA: Seismic Investigation of the Greenland Margin) allow us to address the relative roles of temperature and active upwelling in the North Atlantic on the basis of: (1) precise crustal velocity control on transects spanning an entire rifted margin, allowing mean crustal composition to be estimated; (2) systematic conjugate margin coverage at variable offset from the Iceland hotspot track; and (3) critical in situ geochemical and geochronological data, including samples from deep ocean drilling. The SIGMA data suggest a relatively modest thermal anomaly (100°C) and that active upwelling, probably associated with a rising plume head, strongly contributed to breakup magmatism near

the plume track. Active upwelling continued along the Iceland hotspot track and contributes to melting beneath present-day Iceland. By assuming passive upwelling, prior studies may have significantly overestimated mantle temperatures in the Iceland hotspot and along the margin during continental breakup.

2. Experiment design and data modeling

In order to assess the temporal and spatial evo-

lution of the breakup melting anomaly, we acquired high-precision, crustal-scale, wide-angle seismic data along four profiles situated at various offsets from the Iceland hotspot track (Fig. 1). Line 1 extended along the entire Greenland–Iceland Ridge (GIR) to measure post-breakup magmatism produced by the Iceland hotspot. The southernmost profile, Line 4, crossed the southern tip of Greenland, 1050 km from the hotspot track. Profiles were located to provide in situ sample control from drillholes into the upper crust (e.g., [9]) as well as to lie in approximately con-

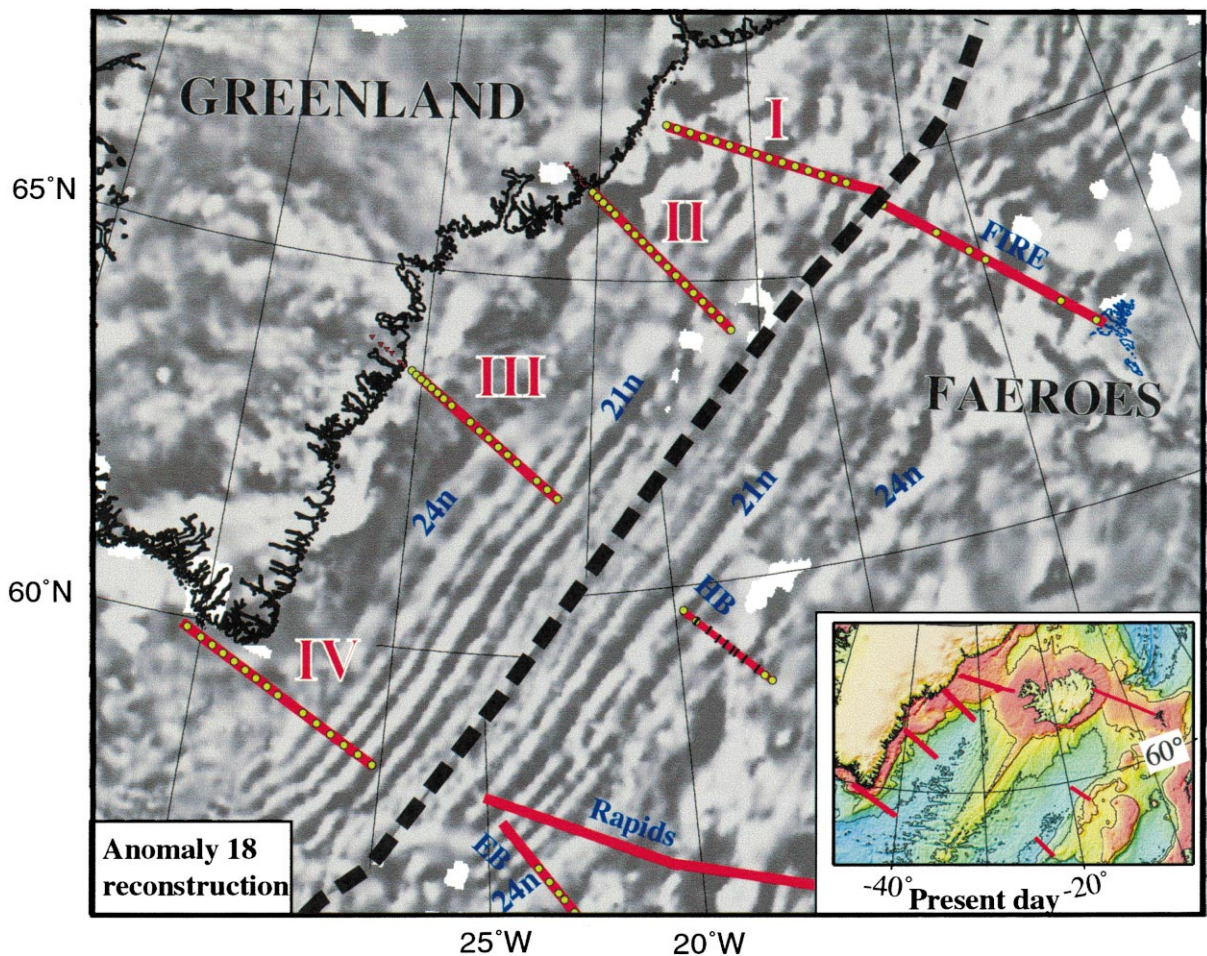


Fig. 1. Location of SIGMA seismic profiles 1–4 and profiles on the conjugate Faeroe–Hatton–Rockall margins, on an anomaly 18 (~40 Ma) reconstruction of the North Atlantic. Shading represents positive (light) and negative (dark) magnetic anomalies [59]; anomalies 21n and 24n are labeled. FIRE, Faeroe–Iceland Ridge Experiment [34]; HB, Hatton Bank [2,20]; EB, Edoras Bank [26]; Rapids, [46]. Inset shows profile locations on present-day bathymetry. Circles represent ocean-bottom seismic instruments; short solid lines represent expanding spread profiles on the HB transect.

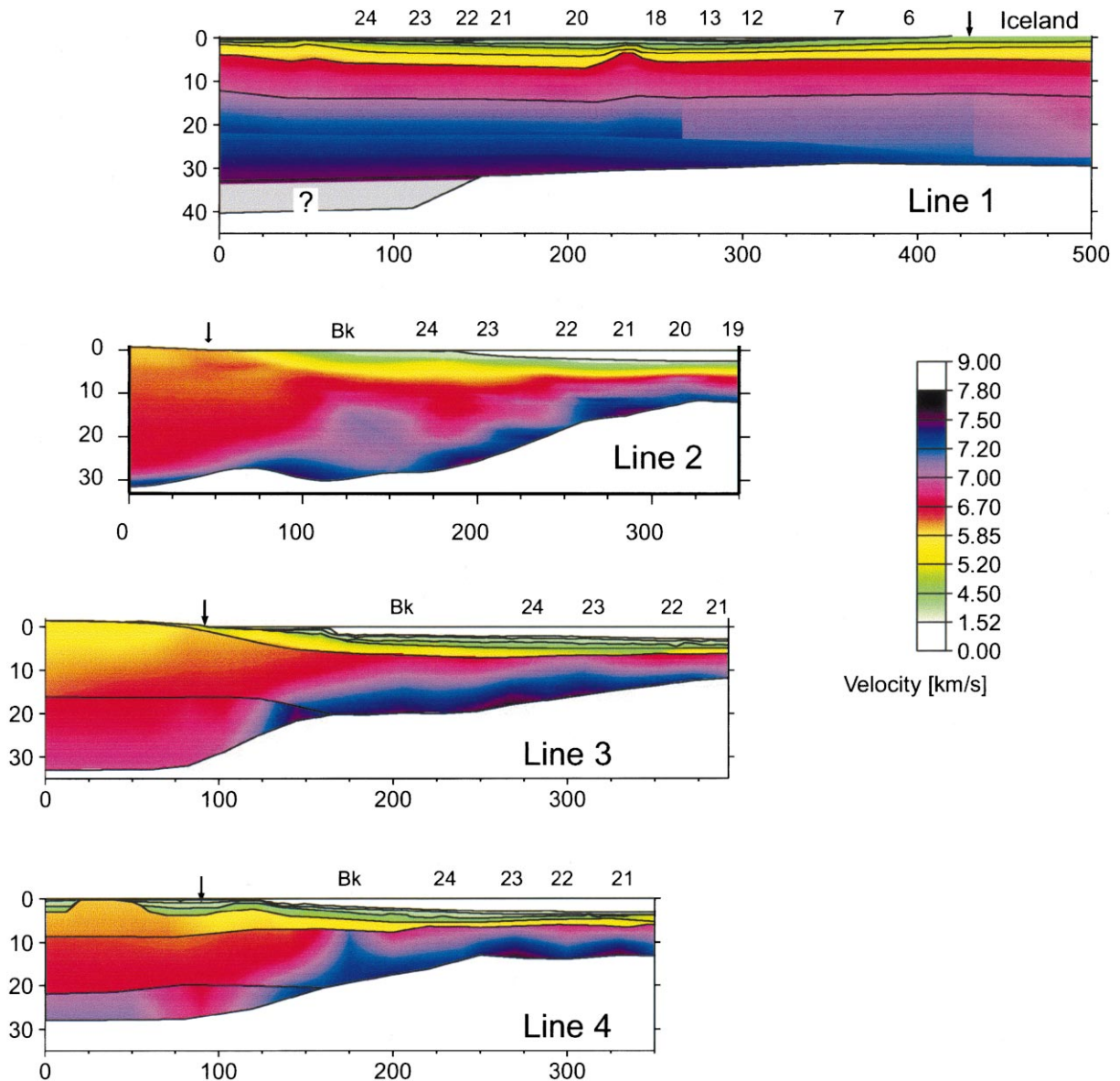


Fig. 2. P-wave velocity models for the four SIGMA transects. Horizontal and vertical scales in km. Arrows show coastlines (projected on Line 4). Numbers along top of models (e.g., 24, 23, etc.) are magnetic anomalies; Bk, interpreted breakup position (100% igneous crust). Color bar shows P-velocity values in km/s. Transect 2 published as Plate 1 in Korenaga et al. [36].

jugate positions to seismic profiles on the Faeroe–Rockall–Hatton margin (Fig. 1; [2,26,34]). Data were acquired using the R/V *Maurice Ewing*, with a 20-element, 137-l airgun array as a source and three sets of recording instruments: the *Ewing*'s 4.0-km-long hydrophone streamer, ocean-bottom seismic hydrophones and seismometers (64 total

stations), and Reftek portable seismometers deployed on Greenland and Iceland (Lines 1, 2, and 3; 20 stations total).

The resulting data set was processed into stacked multichannel seismic (MCS) sections (not reported on here) and wide-angle record sections for all four profiles. Wide-angle data pro-

cessing included instrument relocation, bandpass filtering (4–16 Hz), previous shot noise suppression, and spiking deconvolution. P-wave velocity models (Fig. 2) were derived by inverting travel times of refractions and wide-angle reflections recorded on the ocean-bottom instruments and on-shore seismometers [35,36]. Tight constraints on crustal velocities and thicknesses were provided by refractions and wide-angle reflections observed on the ocean-bottom instruments. Vertical-incidence reflections from the MCS stacks were jointly inverted with wide-angle traveltimes to constrain sediment thickness. Data quality and seismic ray coverage of the wide-angle data are excellent on all four profiles (Fig. 3; [36]). Data from Transect 2 are published [36]; manuscripts detailing data from the other three transects are in preparation.

3. Magmatism on the Southeast Greenland margin

3.1. Thickness of igneous crust

The wide occurrence of thick igneous crust, including high-velocity lower crust (HVLC) and a thick extrusive layer with systematically seaward-dipping reflectors (Fig. 2), confirms that the Southeast Greenland margin is volcanic along its entire length (e.g., [37]). Seaward-dipping reflections exist beneath much of Line 1, and wedges of seaward-dipping reflections are observed on Lines 2, 3, and 4.

SIGMA-1 shows >30-km-thick crust and lower-crustal velocities as high as 7.4–7.5 km/s extending continuously from Greenland to Iceland; a similar crustal structure is reported beneath Iceland [34,38]. Data from the westernmost seismic receivers indicate that the HVLC extends at least to 33 km depth, and possibly to 40 km, beneath the western end of the line (Fig. 2). Gravity modeling also shows landward crustal thickening near the landward end of SIGMA-1 (Reid et al., in preparation), and a similarly large crustal thickness is reported from a conjugate profile off the Faeroes [34]. However, lack of seismic data from onshore Greenland makes the magnitude and composition of such crustal thickening an unre-

solved question, and unless otherwise stated, we assume a maximum crustal thickness of 33 km along SIGMA-1. Maximum crustal thickness along SIGMA-2, -3, and -4 is less than on SIGMA-1, though still close to 30 km at SIGMA-2. Unlike SIGMA-1, all three southern profiles show rapidly seaward decreasing crustal thickness.

The velocity structures (Fig. 2) of SIGMA-2, -3, and -4 define a compositional change from continental to oceanic crust over a 50- to 70-km-wide transition zone. In this transition zone, lower-crustal P-wave velocities increase from 6.5 to 6.6 km/s below the continent to well over 7 km/s within the HVLC, and upper-crustal velocities decrease from 6.0 to 6.3 in the continental crust to 4–5 km/s offshore. The transition zone and its seaward end (the continent–ocean boundary, COB) are independently defined by drilling and deep seismic reflection data along SIGMA-3 [9,39] to lie about 20 km landward of the shelf break [39]. On SIGMA-1 the lack of an upper-crustal lateral velocity gradient indicates that the COB is located landward of the western end of SIGMA-1, i.e., close to the coast, consistent with coastal exposures of sheeted dyke complexes and layered gabbros within a deformed, gneissic host rock [40,41]. Except for SIGMA-3, the location of the COB (Fig. 2) is 180 ± 10 km landward of the well-defined magnetic anomaly 21n (Fig. 1) on all SIGMA profiles. The age of the COB at SIGMA-1 and 3 is determined through combined $^{40}\text{Ar}/^{39}\text{Ar}$ radiometric age determinations and magnetostratigraphy to follow very shortly after magnetic Chron 25n between 56 and 55.5 Ma [40,42]. Ages seaward of the COB are obtained from seafloor spreading anomalies (Fig. 1).

The variation of magmatism in time and space shows a progressive concentration of magmatism toward the Iceland hotspot track (Fig. 4). On all four transects, peak magmatism occurred during the earliest part of breakup, very close to the COB; on the three southern transects, magmatism declined significantly with time. Two zones are defined: a hotspot-proximal zone (SIGMA-1) with consistently thick (>30 km) crust, and a distal zone (SIGMA-3 and -4) with more modest peak volcanism (18 km) that thins rapidly to 9 km. SIGMA-2 occupies a transition between these

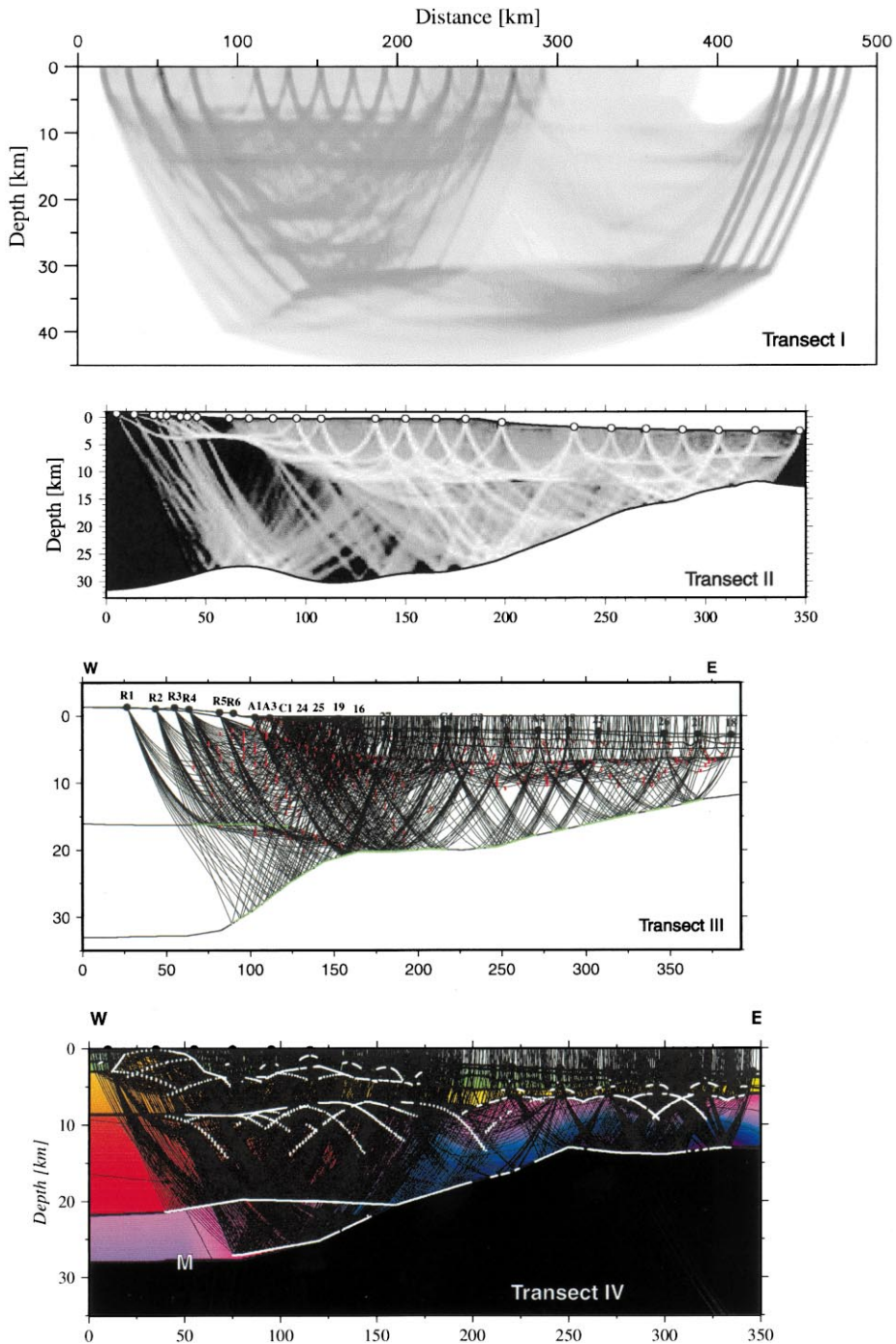


Fig. 3. Ray coverage in the igneous crust on all four profiles. Rays drawn by two-point ray tracing to observed travel time picks. Transect 1 (top) shown as ray density, with darker shades denoting greater ray density. Transect 2 shown as derivative weight sum [36], with lighter shades denoting greater ray density. Transects 3 and 4 show individual rays (solid lines), bottoming points of diving rays (dots), bottoming points of reflections (dots or lines).

two zones: its maximum crustal thickness (~ 30 km) is initially close to that of SIGMA-1 but decreases over 10–12 Myr to only 8–9 km, similar to SIGMA-3 and -4 (Fig. 4). In the distal zone, crustal thickness decays to about 9 km, first (51 Ma) on SIGMA-4, and slightly later (49 Ma) on the more proximal SIGMA-3. Thus, the initially wide melting anomaly (> 1200 km) became restricted to the GIR in only 6 Myr [43].

3.2. Conjugate margin structure

Comparison of three of the SIGMA profiles with profiles in approximately conjugate positions on the British/Faeroe margin shows evidence of both symmetric and asymmetric volcanic margin segments. Crustal thickness variations are symmetric, within error, on two of the three conjugate margin–profile pairs: SIGMA-4/Edoras Bank [26] and SIGMA-1/FIRE [34,44] (Fig. 4). In contrast, the SIGMA-3 profile shows a 150-km-wide zone of thick igneous crust, in contrast to a 50-km-wide zone on the conjugate Hatton Bank profile [19,20] (Fig. 4). Indeed, Larsen and Saunders [39] previously noted an unusually high half-spreading rate near SIGMA-3, and regional studies [45] also suggest asymmetry along this part of the margin. An apparent asymmetry in the timing of peak magmatism (Fig. 4) may be illusory, because magnetic anomaly identification is uncertain at that latitude seaward of Hatton Bank.

This contrast in conjugate structure implies asymmetric spreading at the latitude of SIGMA-3; major ridge jumps after spreading are ruled out by the lack of dip reversals in SDRS on the profile. Two possible explanations would circumvent the conclusion of asymmetric conjugate margin structure. First, the SIGMA-3 and Hatton Bank profiles may not be perfectly conjugate, and their true conjugates might show symmetric structures. This would imply a major transform structure and strong magmatic segmentation along the margin, which is not evident in bathymetric or potential field data. Second, if existing interpretations of the Hatton/Edoras Bank as continental crust are incorrect, the missing magmatic material might be located there. Existing seismic models have limited resolution beneath the axis of the

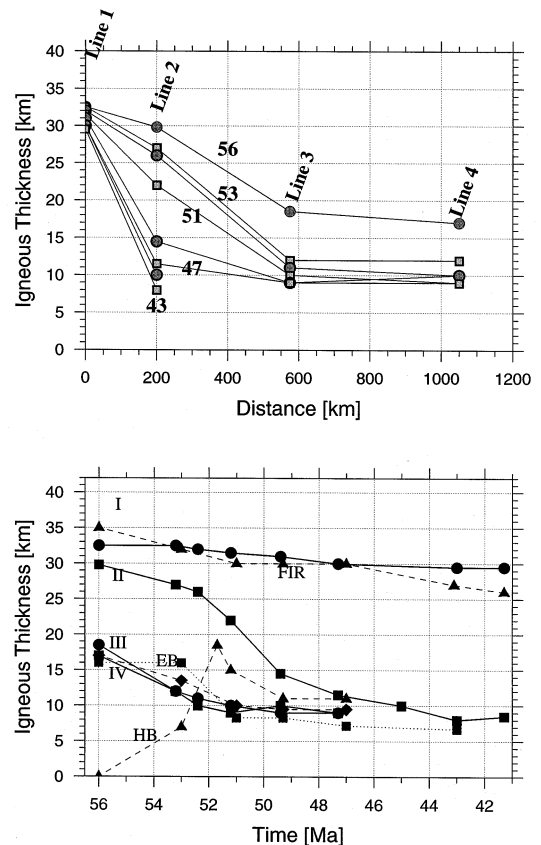


Fig. 4. (Top) Igneous crustal thickness on SIGMA lines plotted as a function of distance from the hotspot track (Line 1). Labeled curves show igneous thickness at different times (56 Ma, 53 Ma, etc.). (Bottom) Igneous crustal thickness on SIGMA transects (solid lines) and profiles on conjugate margins (dashed and dotted lines), plotted as a function of time. Breakup is assumed to occur at 56 Ma. Dashed lines FIR, Faeroe–Iceland Ridge [34]; EB, Edoras Bank [26]; HB, Hatton Bank [2,20]. Dotted line is Rapids profile [46].

Hatton/Edoras Bank; wide-angle lines shot there to date end on the axis and thus do not undershoot the Bank [20,26,46]. Nevertheless, the limited existing seismic data, including an axial expanding spread profile [19], suggest continental crust, and interpreting the Hatton/Edoras Bank as Cenozoic igneous crust would create an asymmetry at the latitude of SIGMA-4/Edoras Bank.

3.3. Magmatic productivity through time

The SIGMA data allow accurate estimates of

magmatic productivity through time in the North Atlantic (Fig. 5). Although the SIGMA-3/Hatton asymmetry is clear (Fig. 5), when conjugate margin pairs are summed, magmatic productivity on the distal transects (SIGMA-3/Hatton and SIGMA-4/Edoras) is identical. Magmatic productivity is two to three times greater in the proximal zone ($\sim 1800 \pm 300 \text{ km}^3/\text{km}/\text{Ma}$) than in the distal zone ($\sim 700 \pm 200 \text{ km}^3/\text{km}/\text{Ma}$) during breakup and twice as great after 42 Ma ($600 \pm 50 \text{ km}^3/\text{km}/\text{Ma}$ vs. $300 \pm 50 \text{ km}^3/\text{km}/\text{Ma}$). Along the distal half of the margin, magmatic productivity is virtually independent of distance from the hotspot track. Decreasing crustal thickness (except on the SIGMA-1/FIRE pair) as well as decreasing spreading rates contribute to the marked decrease in productivity with time (Fig. 5). Errors in productivity come principally from uncertainties in magnetic anomaly correlation and are greatest on Line 1 and during breakup on Line 2. The major features

of Fig. 5, namely, the strong decrease in productivity through time on all transects and the significantly higher productivity in the near-hotspot zone, are robust.

The total volume of thick igneous crust produced along the conjugate margins from (and including) the Iceland hotspot track to south of Greenland between breakup (56 Ma) and anomaly 24n (53 Ma) is $3.7 \times 10^6 \text{ km}^3$; $5.1 \times 10^6 \text{ km}^3$ was produced between breakup and anomaly 23n (51 Ma). Including the margins north of Iceland (e.g., [4]), $9.6 \times 10^6 \text{ km}^3$ of Northeast Atlantic VRM igneous crust formed between breakup and anomaly 23n. This estimate is about 50% greater than reported by Eldholm and Grue [4]. SIGMA profiles and their conjugate counterparts jointly suggest that as much as 70% of this volume lies within the hotspot-proximal zone extending (south of Iceland) to a maximum of 500 km from the center of the hotspot track.

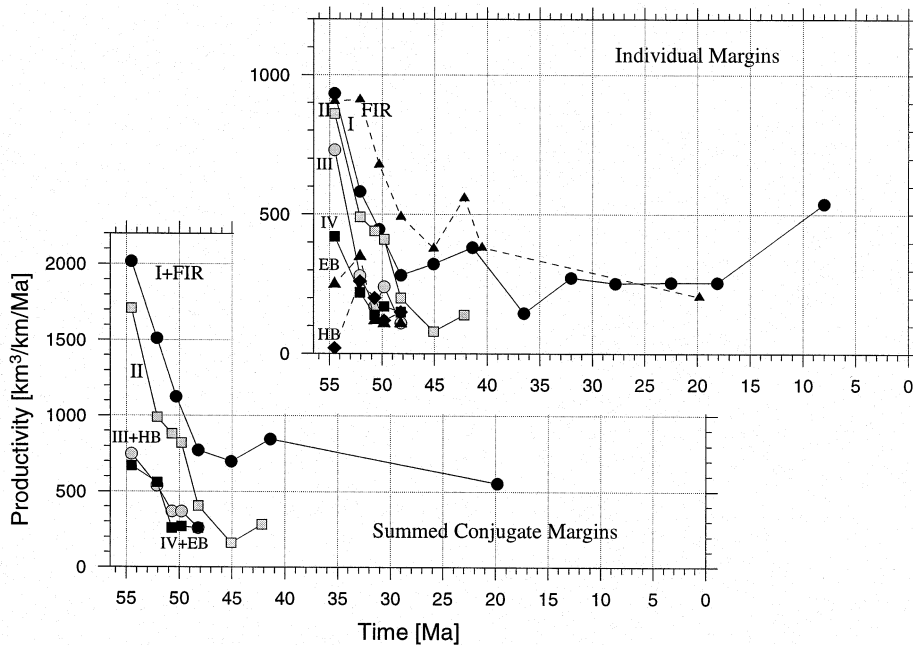


Fig. 5. Magmatic productivity ($\text{km}^3/\text{km}/\text{Ma}$) through time on individual profiles (top) and summed conjugate margins (bottom); SIGMA-2 is assumed to be symmetric with its unsurveyed conjugate. Conjugate Transects III-HB show strong asymmetry in productivity values, but when summed together, show virtually identical productivity to the more symmetric IV-EB conjugate pair. Conjugate margins are assumed to be symmetric at SIGMA Transect II, which lacks a conjugate profile.

4. Melting anomaly: hot or actively upwelling mantle?

Excess magmatism may result from enhanced mantle temperature or active mantle upwelling: higher temperatures increase the fraction of partial melting in the mantle, while active upwelling provides an enhanced flux of mantle through the melting zone. Simple translation of crustal thickness into mantle temperature anomaly may therefore overestimate the temperature by not accounting for active upwelling [7]. However, for a given crustal thickness these two mechanisms produce crust of different major element composition, because the average pressure (P) and fraction (F) of melting differ [13]. Higher potential temperature deepens the solidus and thus increases the height of the melting column, resulting in higher mean P and F and, therefore, melts enriched in MgO and poorer in SiO₂ (e.g., [13]). Active upwelling, in contrast, achieves a given crustal thickness with relatively lower P and F , thus producing melts with lower MgO and higher SiO₂. Such crustal-scale compositional differences would affect the mean seismic velocity of the crust [7] and might therefore be independently constrained with precise crustal velocity control.

We aim to achieve this by comparing observed crustal thickness and mean crustal velocity on the SIGMA transects with the expected velocity–thickness systematics for a common mantle melting model. We calculate the expected crustal thickness (H_c) and mean crustal velocity for a given mantle potential temperature and upwelling ratio (ratio of upwelling flux to spreading half-rate) in the following way. First, we calculate melt fraction at a given pressure along a decompression melting trend at a given potential temperature (Fig. 6) using the adiabatic, equilibrium melting model of McKenzie and Bickle [14]. This model assumes a constant entropy change on melting of 250 J/kg/K and neglects the effect of conductive cooling during rifting [47]. We then use equation 2 of Kelemen and Holbrook [7] to determine mean crustal V_p given the mean pressure and fraction of melting. We assume that all melt is emplaced into the crust and that this is, apart from volatiles, a closed system, with mean

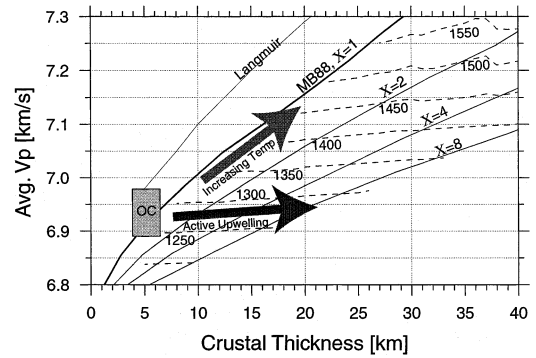


Fig. 6. Predicted mean crustal velocity vs. crustal thickness systematics for two melting models: the Langmuir et al. passive upwelling model (thin line) and the McKenzie and Bickle model, assuming passive upwelling (bold line) and active upwelling ratios (X) of 2, 4, and 8. Dashed lines represent mantle potential temperatures for the McKenzie and Bickle model. OC represents the calculated mean crustal velocity of oceanic crust near the East Pacific Rise [49]. Large arrows represent the isolated effects of increased temperature, which causes increases in both mean crustal velocity and crustal thickness, and increased active upwelling, which causes increasing crustal thickness without a significant change in mean crustal velocity.

crustal composition providing a true representation of the original melt.

Observed mean crustal velocity is calculated from the velocity models (Fig. 2) and corrected to a temperature of 400°C and confining pressure of 600 MPa by applying a pressure correction of 0.00022 km/s/MPa [48] and a temperature correction of -0.0005 km/s/°C. Temperatures are calculated for a conductive geotherm from 10°C at the seafloor to 750°C at 40 km depth. All crustal velocities less than 6.85 km/s are assumed to be affected by alteration or porosity and therefore unrepresentative of bulk composition; these velocities are replaced by 6.85 km/s before applying temperature and pressure corrections. This replacement velocity corresponds, using equation 1 of Kelemen and Holbrook [7], to the representative composition of seaward-dipping wedge basalts sampled on ODP Leg 152 (MgO = 7.5%; SiO₂ = 51%).

These calculations were done for passive upwelling and various extents of active upwelling; the results are referred to below as MB/KH. For

comparison, we also used melt compositions for passive mantle upwelling calculated from the Langmuir et al. fractional melting model [30] to calculate mean crustal V_p . Both the Langmuir and MB/KH models show the same fundamental trend: at a given upwelling ratio, increasing mantle potential temperature causes strong increases in both crustal thickness and velocity (e.g., [3]). However, increasing upwelling ratio at constant potential temperature produces thicker crust with only a slight increase in mean velocity; thus the two variables, temperature and upwelling ratio, produce significantly different trends in the V_p – H_c diagram (Fig. 6). The choice of melting model does not affect these trends but does affect the estimate of absolute temperature: for a given crustal thickness, the fractional melting model of Langmuir et al. [30] predicts mantle potential temperatures about 50°C warmer than the MB/KH passive upwelling model. However, temperature anomalies remain essentially the same. The increase in melt volume is not linearly proportional to upwelling ratio [7], because the final depth of melting is limited by the resultant crustal thickness. The slight increase in average crustal velocity reflects higher mean P induced by a deeper final depth of melt segregation – the ‘lid’ effect of thicker crust.

To test our approach and establish a reference mantle temperature, we applied our method to data from 1-Myr-old, 5.5-km-thick crust at the East Pacific Rise [49]. We applied the same pressure and temperature corrections to the EPR data as to the SIGMA data, except that we assumed an in situ temperature of 500°C at the Moho (6 km subseafloor depth [50]). The calculated mean crustal velocity of 6.96 km/s at the East Pacific Rise is consistent, within error, with the predicted value for passively upwelling mantle with a potential temperature of 1300°C (OC, Fig. 6). Accordingly, we report deviations in mantle temperatures (ΔT) relative to a ‘normal’ temperature of 1300°C.

Data from all SIGMA profiles at breakup plot in the area of above-normal mantle temperature (Fig. 7). On the three southern transects, the velocity/thickness data evolve with time toward lower mantle temperature. Data from SIGMA-3 and SIGMA-4 lie close to the MB/KH passive upwell-

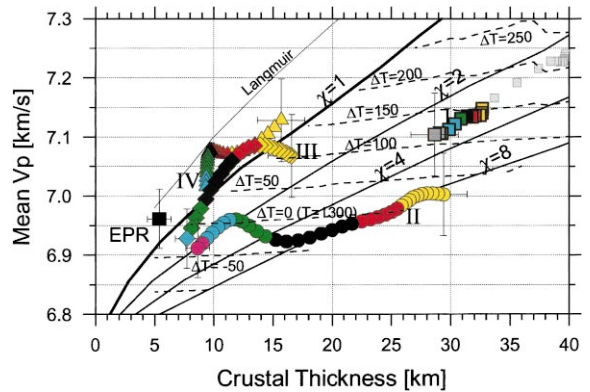


Fig. 7. Mean crustal velocity and crustal thickness data for the four SIGMA profiles (I, squares; II, circles; III, diamonds; IV, triangles) and for oceanic crust near the East Pacific Rise (EPR; [49]). Representative error bars are shown for thick- and thin-crust portions of each line. Melting model systematics as in Fig. 6. Color coding of symbols represents crustal age: yellow = breakup (56 Ma) to anomaly 24 (52.9 Ma); red = anomaly 24 to anomaly 23 (51.2 Ma); dark blue = anomaly 23 to anomaly 22 (49.3 Ma); green = anomaly 22 to anomaly 21 (47.1 Ma); light blue = anomaly 21 to anomaly 20 (43.1 Ma); dark gray = post-anomaly 20. Light gray boxes correspond to alternative Line I model with thick underplate (gray in Fig. 2).

ing curve, whereas SIGMA-1 and SIGMA-2 at breakup lie well in the field of active upwelling (Fig. 7). We conclude that: (1) a margin-wide mantle thermal anomaly was present during breakup but was exhausted beneath most of the margin within 6–12 Myr; (2) active upwelling at ~ 4 –6 times the passive rate (or a process with similar effect) is required near the hotspot track but not in the distal zone, which can be modeled by purely passive upwelling (at $\Delta T = 100 \pm 50^\circ\text{C}$) or with only modestly active upwelling (two times passive); and (3) after breakup, temperatures remain elevated ($\Delta T \sim 100 \pm 50^\circ\text{C}$) on the hotspot track compared to elsewhere ($\Delta T = 25 \pm 50^\circ\text{C}$). A possible along-margin variation in mantle temperature during initial breakup cannot be resolved by our data (although temperatures appear somewhat low on Transect 2), and a uniform $\Delta T = 100 \pm 50^\circ\text{C}$ along the entire margin is permissible. However, if 40-km-thick igneous crust is present at SIGMA-1 (Fig. 2), higher, but rapidly decreasing, temperature (max. $\Delta T = 200 \pm 50^\circ\text{C}$) in

the proximal zone during earliest breakup is indicated (Fig. 7). If a mantle component more fertile than perioditic mantle, e.g., recycled oceanic crust, is present in the Iceland mantle plume, at constant ΔT it would melt to higher degrees than normal mantle, and therefore increase the apparent ratio of active upwelling, though this effect is likely small.

To test the robustness of these conclusions, we conducted extensive error testing of all four profiles to determine ranges of acceptable velocities and crustal thicknesses. Models were tested by systematically varying crustal velocity in starting models and finding best-fit models by inverting for depths to the top of the lower crust and the Moho. Traveltime misfit statistics indicate an uncertainty in mean crustal velocity of ± 0.08 km/s in thick crust and ± 0.05 km/s in thin crust. (Even though individual model parameters may have larger errors, the error in mean crustal velocity is lower, since errors in model parameters are often negatively correlated. That is, increasing the velocity at a lower-crustal node will require a corresponding decrease in an upper-crustal node in order to conserve PmP travel times; mean crustal velocity is thus little affected.) Korenaga et al. [36] conducted an extensive Monte Carlo error analysis for Line 2 and determined a similar uncertainty. Acceptable models have restricted slopes in V_p-H_c space: all acceptable models for Line 2, for example, have a flatter V_p-H_c slope than the passive upwelling curves, implying a decreasing upwelling ratio with time. Forcing SIGMA-1 V_p-H_c data onto the MB/KH passive upwelling curve would require a mean V_p greater than 7.3 km/s, well outside the permissible velocity field. Similarly, SIGMA-3 and -4 cannot be modeled with constant potential temperature. (The only conceivable way of raising the mean crustal velocity on SIGMA-1 to values consistent with passive upwelling would be to postulate a 15-km-thick layer of cumulate olivine of velocity 8.0 km/s; the implied crustal thickness would be 45 km, much greater than any published estimate, and the implied ΔT would be $> 350^\circ\text{C}$, which is inconsistent with the chemistry of Iceland lavas [13].)

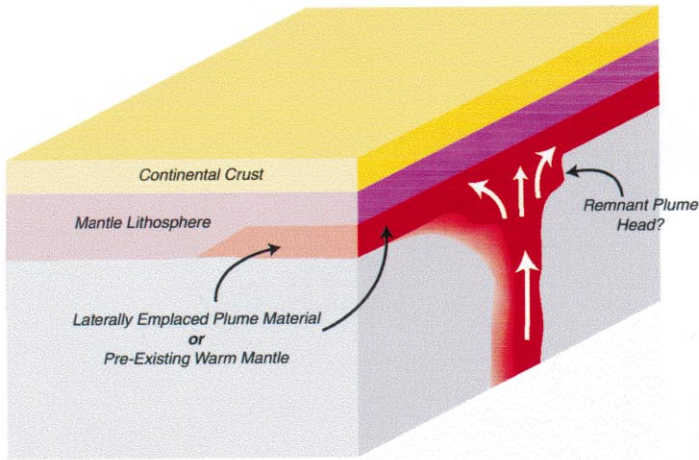
5. Implications for volcanic margin genesis

The SIGMA data show that the thermal anomaly associated with the breakup of Greenland from Europe was modest ($\sim 100 \pm 50^\circ\text{C}$), relatively uniform along the margin, and transient. The thick crust (> 30 km) and relatively low mean crustal P-velocity (~ 7.1 km/s) along the entire Iceland plume track suggests that active upwelling occurs above the present-day Iceland plume, and that a similar process has occurred during the entire history of the plume, at least since breakup at ~ 56 Ma. The active upwelling associated with plume passage through the deeper mantle thus continues into the shallow levels of decompression melting within extensional rifts.

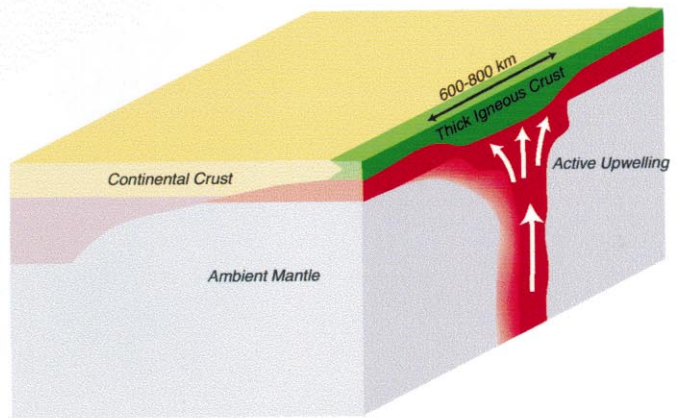
The requirement for an Iceland melting anomaly at early breakup implies that acceptable models for the formation of the Northeast Atlantic VRM must include the proto-Icelandic plume. Two types of pure plume models are consistent with our findings: the low-viscosity, thin plume head of Sleep [51] and Larsen and Saunders [39] and the plume incubation models, in which the Iceland plume ponded beneath the Greenland continental lithosphere long before rifting. In addition, models in which the entire margin was underlain by a thermal anomaly due to continental insulation (e.g., [52]), with an additional active upwelling provided by the Iceland hotspot, are equally consistent with our data. However, the contrast between largely amagmatic Cretaceous rifting (e.g., [53]) and widespread, virtually isochronous basaltic magmatism at 61 ± 1.5 Ma (e.g., [42,54]) strongly suggests that the thermal conditions of the asthenospheric mantle changed as a result of a sudden plume impact rather than long-standing plume incubation.

Regardless of the origin of the thermal anomaly, the pattern of active upwelling provided by our data yields insight into the evolution of melting dynamics during continental breakup in the North Atlantic. If we adopt the plume impact model, then the SIGMA data provide a map of the evolution of the impacting plume head. We suggest that the region of strongly active upwelling marks the extent of the rising plume head, where a vertical component of motion in upwell-

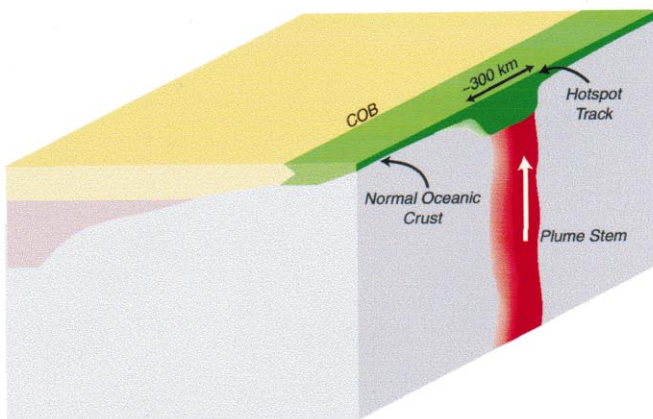
Pre-Breakup



Breakup (~55 Ma)



Seafloor Spreading (~45 Ma)



ing plume material increases flux through the melting zone. At breakup, the actively upwelling part of the plume extended at least to SIGMA-2 but not as far south as SIGMA-3. The rising plume head at breakup is thus constrained to be between 200 and 500 km in radius.

The distal parts of the margin require little or no active upwelling. In these regions, warm material, possibly originating from the plume head, was laterally emplaced (e.g., [27]) but lacked a vertical component of motion in excess of the passive upwelling velocity. Distal-zone magmatism was enhanced by excess temperature ($\sim 100^\circ\text{C}$) but still fell short of magmatism in the proximal zone, where strongly active upwelling occurred. The modest temperature anomaly appears to conflict with picritic lavas (up to $>20\%$ MgO) on the distal margins, which have been interpreted to represent high degree melts from a high temperature source ($\Delta T = 250^\circ\text{C}$; e.g., [54]). However, the downward increase in crustal velocities on SIGMA-3 from 7.1 km/s to 7.4 km/s indicates that the high-MgO picrites most likely represent lower-crustal cumulate material rather than primary melts. Low-MgO picrites and olivine basalts (12–14% MgO) sample near SIGMA-3 fit the mean V_p data and therefore are likely to represent the primary, unfractionated melt compositions.

A scenario consistent with our results is as follows (Fig. 8): A plume of radius ~ 300 km and ΔT of $\sim 125^\circ\text{C}$ impacted the margin around 61 Ma and laterally delivered warm material from its upper portions to more distal portions of the margin (e.g., [27]). At breakup (56 Ma), the lower half of the plume head continued to feed active upwelling into the proximal portion of the margin. By 45 Ma, both the remaining plume head and the distal warm layer were exhausted, and excess magmatism was largely confined to a narrow

(< 200 km radius) zone immediately above the Iceland plume stem.

This model of VRM genesis differs from previous models in several important respects. First, the inclusion of active upwelling provides a mechanism for enhancing volcanism with only modest thermal anomalies. Barton and White [26], lacking constraints on active upwelling, interpreted a mantle potential temperature of 1550°C ($\Delta T = 250^\circ\text{C}$) for the 30-km-thick crust on the Faeroe–Iceland Ridge and about 100°C cooler for the thinner crust far to the south. In contrast, our inference of an active upwelling ratio of ~ 4 yields a temperature anomaly of only $125 \pm 50^\circ\text{C}$ for the 30–33-km-thick crust beneath the conjugate GIR and little or no along-margin temperature variation (Fig. 7). This inferred cooler temperature is consistent with inversion of trace element concentrations from drill cores along SIGMA-3, which suggest a mantle thermal anomaly of about 100°C [55]. Active upwelling and enhanced temperature were transient along SIGMA-2 but constant along the entire GIR. We therefore reject the notion of a margin-wide melting anomaly caused solely by active mantle upwelling in response to rifting, without a temperature anomaly (e.g., [16]). On the contrary, strongly active upwelling, where indicated by our data, is hotspot-related. Our results agree with the recent geodynamical models of Keen and Boutillier [33], who inferred a thin, moderately hot (1450°C) layer beneath the margin and transient active upwelling during breakup. Although Keen and Boutillier infer active upwelling in the distal region, where we infer nearly passive upwelling, our data are compatible with modestly active upwelling there (Fig. 7). Models of sheet-like upwellings that impact the margin [26] are inconsistent with our data, since such models would predict strongly active upwelling

←

Fig. 8. Conceptual cartoon of a plume-impact scenario consistent with our results. Prior to breakup, a rising plume head ($\Delta T = 125^\circ\text{C}$) impacts the continental lithosphere and spreads laterally to emplace warm material beneath the continent. At breakup (56 Ma), strongly active upwelling (white arrows) occurs above remnant plume head and plume stem, building 30-km-thick igneous crust in the hotspot-proximal region, while passively upwelling mantle yields 18-km-thick igneous crust in the distal region. Finally, at 45 Ma, the warm mantle reservoir has been exhausted, and excess magmatism is strongly focused above the plume stem. An alternative, steady-state hotspot scenario, which is allowable by our data, would require a pre-existing warm upper mantle unrelated to the plume.

along whole margin. Finally, numerical models of the present-day Iceland plume range from those that include active upwelling but overestimate crustal thickness [56,57] to others [58] that match crustal thickness data with a hot (1530°C), narrow plume (radius 100 km). Our results suggest that future numerical models must incorporate mean crustal velocity as a constraint on the relative roles of active upwelling and enhanced temperatures.

An important result of our work is the demonstration that active upwelling in the melting zone occurred both during continental breakup and, later, above the steady-state Iceland plume. Previous estimates of mantle potential temperature anomalies from crustal thickness have neglected this. Thus, incorporation of active upwelling explains the apparently paradoxical result that the breakup-related, thick igneous crust in the North Atlantic has a 50% greater volume than previously thought, despite a mantle thermal anomaly that is only half as large as in most previous models.

Acknowledgements

We thank the captain and crew of the R/V *Ewing* for their hard work during a long and difficult cruise. We thank B. Brandsdottir, R.S. White and the Cambridge team for deployment of seismometers on Iceland. The data quality owes much to the field efforts of Jim Dolan, David DuBois, Rob Handy, Bob Busby, Paul Henkart, Anders Brun, Thomas Nielsen, and Bill Koperwhats. This work was supported by National Science Foundation Grant OCE-9416631. [RV]

References

- [1] J.C. Mutter, M. Talwani, P.L. Stoffa, Origin of seaward-dipping reflectors in oceanic crust off the Norwegian margin by 'subaerial sea-floor spreading', *Geology* 10 (1982) 353–357.
- [2] R.S. White, G.D. Spence, S.R. Fowler, D.P. McKenzie, G.K. Westbrook, A.N. Bowen, Magmatism at rifted continental margins, *Nature* 330 (1987) 439–444.
- [3] R. White, D. McKenzie, Magmatism at rift zones: The generation of volcanic continental margins and flood basalts, *J. Geophys. Res.* 94 (1989) 7685–7729.
- [4] O. Eldholm, K. Grue, North Atlantic volcanic margins: Dimensions and production rates, *J. Geophys. Res.* 99 (1994) 2955–2968.
- [5] T.P. Gladchenko, K. Hinz, O. Eldholm, H. Meyer, S. Neben, J. Skogseid, South Atlantic volcanic margins, *J. Geol. Soc. Lond.* 154 (1997) 465–470.
- [6] W.S. Holbrook, P.B. Kelemen, Large igneous province on the U.S. Atlantic margin and implications for magmatism during continental breakup, *Nature* 364 (1993) 433–436.
- [7] P.B. Kelemen, W.S. Holbrook, Origin of thick, high-velocity crust along the US East Coast margin, *J. Geophys. Res.* 100 (1995) 10077–10094.
- [8] K. Hinz, A hypothesis on terrestrial catastrophes wedges of very thick oceanward dipping layers beneath passive margins, *Geol. Jahrb.* 22 (1981) 5–28.
- [9] H.C. Larsen, A.D. Saunders, P. Clift (Eds.), *Proc. ODP, Init. Rep.*, 152 (Pt. 1), Ocean Drilling Program, College Station, TX, 1994.
- [10] D.G. Roberts, J. Backman, A.C. Moarton, J.W. Murray, J.B. Keene, Evolution of volcanic rifted margins Synthesis of Leg 81 results on the west margin of Rockall Plateau, *Init. Rep. Deep Sea Dril. Proj.* 81 (1984) 883–911.
- [11] O. Eldholm, J. Thiede, O.L.S. Party, Formation of the Norwegian Sea, *Nature* 319 (1986) 360–361.
- [12] The MELT Seismic Team., Imaging the deep seismic structure beneath a mid-ocean ridge: The MELT experiment, *Science* 280 (1998) 1215–1218.
- [13] E.M. Klein, C.H. Langmuir, Global correlations of ocean ridge basalt chemistry with axial depth and crustal thickness, *J. Geophys. Res.* 92 (1987) 8089–8115.
- [14] D. McKenzie, M.J. Bickle, The volume and composition of melt generated by extension of the lithosphere, *J. Petrol.* 29 (1988) 625–679.
- [15] C.E. Keen, C. Beaumont, Geodynamics of rifted continental margins, in: M.J. Keen, G.L. Williams (Eds.), *Geology of the Continental Margin of Eastern Canada, The Geology of North America, v. I-1*, Geological Society of America, 1990, pp. 391–472.
- [16] J.C. Mutter, W.R. Buck, C.M. Zehnder, Convective partial melting 1. A model for the formation of thick basaltic sequences during the initiation of spreading, *J. Geophys. Res.* 93 (1988) 1031–1048.
- [17] W.A. Deer, Tertiary igneous rocks between Scoresby Sund and Kap Gustav Holm, East Greenland, in: A. Escher, W.S. Watt (Eds.), *Geology of Greenland, Grønlands Geologiske Undersøgelse*, Copenhagen, 1976, pp. 404–429.
- [18] R. Waagstein, Structure, composition and age of the Faeroe basalt plateau, in: A.C. Morton, L.M. Parson, (Eds.), *Early Tertiary Volcanism and the Opening of the NE Atlantic*, *Geol. Soc. Spec. Publ.* 39, Blackwell Scientific, Oxford, 1988, pp. 225–238.
- [19] S.R. Fowler, R.S. White, G.D. Spence, G.K. Westbrook,

- The Hatton Bank continental margin – II. Deep structure from two-ship expanding spread seismic profiles, *Geophys. J. Int.* 96 (1989) 295–309.
- [20] J.V. Morgan, P.J. Barton, R.S. White, The Hatton Bank continental margin – III. Structure from wide-angle OBS and multichannel seismic refraction profiles, *Geophys. J. Int.* 98 (1989) 367–384.
- [21] J.C. Mutter, M. Talwani, P.L. Stoffa, Evidence for a thick oceanic crust adjacent to the Norwegian margin, *J. Geophys. Res.* 89 (1984) 483–502.
- [22] R.C. Courtney, R.S. White, Anomalous heat flow and geoid across the Cape Verde Rise: evidence for dynamic support from a thermal plume in the mantle, *Geophys. J. R. Astron. Soc.* 87 (1986) 815–867.
- [23] R.S. White, Initiation of the Iceland plume and opening of the North Atlantic, in: A.J. Tankard, H.R. Balkwill (Eds.), *Extension Tectonics and Stratigraphy of the North Atlantic Margins*, AAPG Memoir 46, Tulsa, OK, 1989, pp. 149–154.
- [24] I.H. Campbell, R.W. Griffiths, Implications of mantle plume structure for the evolution of flood basalts, *Earth Planet. Sci. Lett.* 99 (1990) 79–93.
- [25] R.S. White, D. McKenzie, Mantle plumes and flood basalts, *J. Geophys. Res.* 100 (1995) 17543–17585.
- [26] A.J. Barton, R.S. White, Crustal structure of the Edoras Bank margin and mantle thermal anomalies beneath the North Atlantic, *J. Geophys. Res.* 102 (1997) 3109–3129.
- [27] N.H. Sleep, Lateral flow of hot plume material ponded at sublithospheric depths, *J. Geophys. Res.* 101 (1996) 28065–28083.
- [28] D.L. Anderson, Superplumes or supercontinents?, *Geology* 22 (1994) 39–42.
- [29] M. Gurnis, Large-scale mantle convection and the aggregation and dispersal of supercontinents, *Nature* 332 (1988) 695–699.
- [30] C.H. Langmuir, E.M. Klein, T. Plank, Petrological constraints on melt formation and migration beneath mid-ocean ridges, in: J. Phipps Morgan, D. Blackman, J.L. Sinton (Eds.), *Mantle Flow and Melt Generation at Mid-Ocean Ridges* (Geophys. Monogr. h 71), American Geophysical Union, Washington, DC, 1992, pp. 183–280.
- [31] D.L. Turcotte, J. Phipps Morgan, The physics of magma migration and mantle flow beneath a mid-ocean ridge, in: J. Phipps Morgan, D. Blackman, J.L. Sinton, (Eds.), *Mantle Flow and Melt Generation at Mid-Ocean Ridges* (Geophys. Monogr. 71), American Geophysical Union, Washington, DC, 1992, pp. 155–182.
- [32] R.R. Boutilier, C.E. Keen, Small-scale convection and divergent plate boundaries, *J. Geophys. Res.* 104 (1999) 7389–7403.
- [33] C.E. Keen, R.R. Boutilier, The interaction of rifting and hot horizontal plume sheets at volcanic margins, *J. Geophys. Res.* 105 (2000) 13375–13387.
- [34] J.R. Smallwood, R.K. Staples, K.R. Richardson, R.S. White FIRE Working Group., Structure and development of the crust above the Iceland mantle plume: from continental rift to oceanic spreading center, *J. Geophys. Res.* 104 (1999) 22885–22902.
- [35] C.A. Zelt, R.B. Smith, Seismic traveltime inversion for 2-D crustal velocity structure, *Geophys. J. Int.* 108 (1992) 16–34.
- [36] J. Korenaga, W.S. Holbrook, G.M. Kent, P.B. Kelemen, R.S. Detrick, H.-C. Larsen, J.R. Hopper, T. Dahl-Jensen, Crustal structure of the Southeast Greenland margin from joint refraction and reflection seismic tomography, *J. Geophys. Res.* 105 (2000) 21591–21614.
- [37] H.C. Larsen, S. Jakobsdóttir, Distribution, crustal properties and significance of seawards-dipping sub-basement reflectors off E Greenland, in: A.C. Morton, L.M. Parson (Eds.), *Early Tertiary Volcanism and the Opening of the NE Atlantic*, Geological Society Special Publication no. 39, Blackwell Scientific, Oxford, 1988, pp. 95–114.
- [38] R.K. Staples, R.S. White, B. Brandsdóttir, W.H. Menke, P.K.H. Maguire, J. McBride, Faroe–Iceland Ridge experiment – I. The crustal structure of north-eastern Iceland, *J. Geophys. Res.* 102 (1997) 7867–7886.
- [39] H.C. Larsen, A.D. Saunders, Tectonism and volcanism at the SE Greenland rifted margin: A record of plume impact and later continental rupture, in: A.D. Saunders, H.C. Larsen, S. Wise (Eds.), *Proc. ODP, Sci. Res. 152*, Ocean Drilling Program, College Station, TX, 1998, in press.
- [40] C. Tegner, R.A. Duncan, S.B. Bernstein, C.K. Brooks, D.K. Bird, M. Storey, 40Ar/39Ar geochronology of Tertiary mafic intrusions along the East Greenland rifted margin: Relation to flood basalts and the Iceland hotspot track, *Earth Planet. Sci. Lett.* 156 (1998) 75–88.
- [41] J.A. Karson, C.K. Brooks, Structural and magmatic segmentation of the Tertiary East Greenland volcanic rifted margin, in: P. Ryan, C. MacNiocail (Eds.), *Continental Tectonics*, Geological Society of London, Special Publication, London, 1999.
- [42] M. Storey, R.A. Duncan, A.K. Pedersen, L.M. Larsen, H.C. Larsen, 40Ar/39Ar geochronology of the West Greenland Tertiary volcanic province, *Earth Planet. Sci. Lett.* 160 (1998) 569–586.
- [43] C.J. Wolfe, I.T. Bjarnasson, J.C. VanDecar, S.C. Solomon, Seismic structure of the Iceland mantle plume, *Nature* 385 (1997) 245–247.
- [44] K.R. Richardson, J.R. Smallwood, R.S. White, D. Snyder, P.K.H. Maguire, Crustal structure beneath the Faroe Islands and the Faroe–Iceland Ridge, *Tectonophysics* 300 (1998) 159–180.
- [45] R.D. Müller, W.R. Roest, J.-Y. Royer, Asymmetric sea-floor spreading caused by ridge–plume interactions, *Nature* 396 (1998) 455–459.
- [46] U. Vogt, J. Makris, B.M. O’Reilly, F. Hauser, P.W. Readman, A.W.B. Jacob, P.M. Shannon, The Hatton Basin and continental margin: Crustal structure from wide-angle seismic and gravity data, *J. Geophys. Res.* 103 (1998) 12545–12566.
- [47] J.W. Bown, R.S. White, The effect of finite duration ex-

- tension on melt generation at rifted continental margins, *J. Geophys. Res.* 100 (1995) 18011–18029.
- [48] N.I. Christensen, W.D. Mooney, Seismic velocity structure and composition of the continental crust: A global view, *J. Geophys. Res.* 100 (1995) 9761–9788.
- [49] J.P. Canales, R.S. Detrick, S. Bazin, A.J. Harding, J. Orcutt, Off-axis crustal thickness across and along the East Pacific Rise within the MELT area, *Science* 280 (1998) 1218–1221.
- [50] C.A. Stein, S. Stein, A model for the global variation in oceanic depth and heat flow with lithospheric age, *Nature* 359 (1992) 123–129.
- [51] N.H. Sleep, Hotspots and mantle plumes: Some phenomenology, *J. Geophys. Res.* 95 (1990) 6715–6736.
- [52] D.L. Anderson, The sublithospheric mantle as the source of continental flood basalts; the case against the continental lithosphere and plume head reservoirs, *Earth Planet. Sci. Lett.* 123 (1994) 269–280.
- [53] J.A. Chalmers, T.C.R. Pulvertaft, F.G. Christiansen, H.C. Larsen, K.H. Laursen, T.G. Ottesen, The southern West Greenland continental margin; rifting history, basin development, and petroleum potential, in: J.R. Parker (Ed.), *Petroleum geology of Northwest Europe*, Proc. 4th Conf., Geological Society of London, London, 1993, pp. 915–931.
- [54] A.D. Saunders, J.G. Fitton, A.C. Kerr, M.J. Norry, R.W. Kent, The North Atlantic igneous province, in: J.J. Mahoney, M. Coffin (Eds.), *Large igneous provinces*, American Geophysical Union, Washington, DC, 1997, pp. 45–94.
- [55] M.S. Fram, C.E. Leshner, A.M. Volpe, Mantle melting systematics: The transition from continental to oceanic volcanism on the Southeast Greenland margin, in: H.C. Larsen, A. Saunders, P. Clift (Eds.), *Proc. Ocean Drilling Program Sci. Results*, v. 152, Ocean Drilling Program, College Station, TX, 1998.
- [56] N. Ribe, U.R. Christensen, J. Theissing, The dynamics of plume–ridge interaction, 1: Ridge-centered plumes, *Earth Planet. Sci. Lett.* 134 (1995) 155–168.
- [57] G. Ito, J. Lin, C.W. Gable, Dynamics of mantle flow and melting at a ridge-centered hotspot Iceland and the Mid-Atlantic Ridge, *Earth Planet. Sci. Lett.* 144 (1996) 53–74.
- [58] G. Ito, Y. Shen, G. Hirth, C.J. Wolfe, Mantle flow, melting, and dehydration of the Iceland mantle plume, *Earth Planet. Sci. Lett.* 165 (1999) 81–96.
- [59] R. Macnab, J. Verhoef, W. Roest, J. Arkani-Hamed, New database documents the magnetic character of the Arctic and North Atlantic, *Eos Trans. Am. Geophys. Union* 76 (1995) 449–458.